Molecular Therapy
Original Article

Proof-of-concept for multiple AON delivery by a single U7snRNA vector to restore splicing defects in *ABCA4*

Nuria Suárez-Herrera,[1] Iris B. Riswick,[1] Irene Vázquez-Domínguez,[1] Lonneke Duijkers,[1] Dyah W. Karjosukarso,[1] Davide Piccolo,[2] Miriam Bauwens,[3,4] Elfride De Baere,[3,4] Michael E. Cheetham,[2] Alejandro Garanto,[1,5] and Rob W.J. Collin[1]

[1]Radboud University Medical Center, Department of Human Genetics, 6525GA Nijmegen, the Netherlands; [2]UCL Institute of Ophthalmology, London EC1V 9EL, UK; [3]Department of Biomolecular Medicine, Ghent University, 9000 Ghent, Belgium; [4]Center for Medical Genetics, Ghent University Hospital, 9000 Ghent, Belgium; [5]Radboud University Medical Center, Amalia Children's Hospital, Department of Pediatrics, Nijmegen 6252GA, the Netherlands

The high allelic heterogeneity in Stargardt disease (STGD1) complicates the design of intervention strategies. A significant proportion of pathogenic intronic *ABCA4* variants alters the pre-mRNA splicing process. Antisense oligonucleotides (AONs) are an attractive yet mutation-specific therapeutic strategy to restore these splicing defects. In this study, we experimentally assessed the potential of a splicing modulation therapy to target multiple intronic *ABCA4* variants. AONs were inserted into U7snRNA gene cassettes and tested in midigene-based splice assays. Five potent antisense sequences were selected to generate a multiple U7snRNA cassette construct, and this combination vector showed substantial rescue of all of the splicing defects. Therefore, the combination cassette was used for viral synthesis and assessment in patient-derived photoreceptor precursor cells (PPCs). Simultaneous delivery of several modified U7snRNAs through a single AAV, however, did not show substantial splicing correction, probably due to suboptimal transduction efficiency in PPCs and/or a heterogeneous viral population containing incomplete AAV genomes. Overall, these data demonstrate the potential of the U7snRNA system to rescue multiple splicing defects, but also suggest that AAV-associated challenges are still a limiting step, underscoring the need for further optimization before implementing this strategy as a potential treatment for STGD1.

INTRODUCTION

Inherited retinal diseases (IRDs) are a heterogeneous group of conditions in which the affected individuals experience progressive and significant vision loss. This group can be divided into several categories depending on their clinical features and progression of symptoms. Macular dystrophies are characterized by a progressive bilateral impairment of central vision.[1,2] Stargardt disease type 1 (STGD1; OMIM: 248200) is the most common macular dystrophy,[3] affecting 1 in every 8,000 to 10,000 individuals worldwide and commonly appearing during adolescence or young adulthood.[4,5] STGD1 is caused by biallelic mutations in the *ABCA4* gene, which encodes the ATP-binding cassette type A4 transporter. This transmembrane protein is localized at the rim region of the photoreceptor outer segment discs and it is important for the visual cycle. Impairment of ABCA4 activity enhances the accumulation of toxic retinoid by-products in retinal pigment epithelium (RPE) cells, eventually leading to photoreceptor cell degeneration and progressive vision loss.[6,7] In-depth sequencing of the *ABCA4* locus has revealed enormous allelic heterogeneity in disease-causing variants within the STGD1 patient population over the last 10 years.[8–17] In total, there are more than 2,400 uniquely reported *ABCA4* variants (www.lovd.nl/ABCA4), a number that is constantly increasing as new cohorts are screened. A significant proportion of these variants negatively affect the pre-mRNA splicing process. Within this group, there are many variants that activate splice sites or enhancers within an intron that lead to pseudoexon (PE) insertions into *ABCA4* mRNA transcripts.[5]

STGD1 still represents a challenge in terms of therapy design due to its high allelic heterogeneity and the large size of *ABCA4* cDNA (6.8 kb), which is too large for conventional adeno-associated virus (AAV)–mediated gene augmentation. Antisense oligonucleotide (AON)–based splicing modulation is a promising strategy to restore pre-mRNA splicing.[18–21] AONs are small modified RNA molecules that can alter splicing at the pre-mRNA level and correct potential aberrant splicing via sequence-specific binding and steric blockage of splicing machinery components, among other mechanisms.[22] Until now, the design of AONs aimed to individually target intronic *ABCA4* variants and assess the rescue independently.[11,12,15,17,23–25] Consequently, this requires the development of an individual treatment for each patient group harboring a specific intronic *ABCA4* variant, which generally is a costly and time-consuming process. Because each AON targets a relatively small group of STGD1 patients

Received 13 September 2023; accepted 12 January 2024;
https://doi.org/10.1016/j.ymthe.2024.01.019.

Correspondence: Rob W.J. Collin, Radboud University Medical Center, Department of Human Genetics, 6525GA Nijmegen, the Netherlands.
E-mail: rob.collin@radboudumc.nl

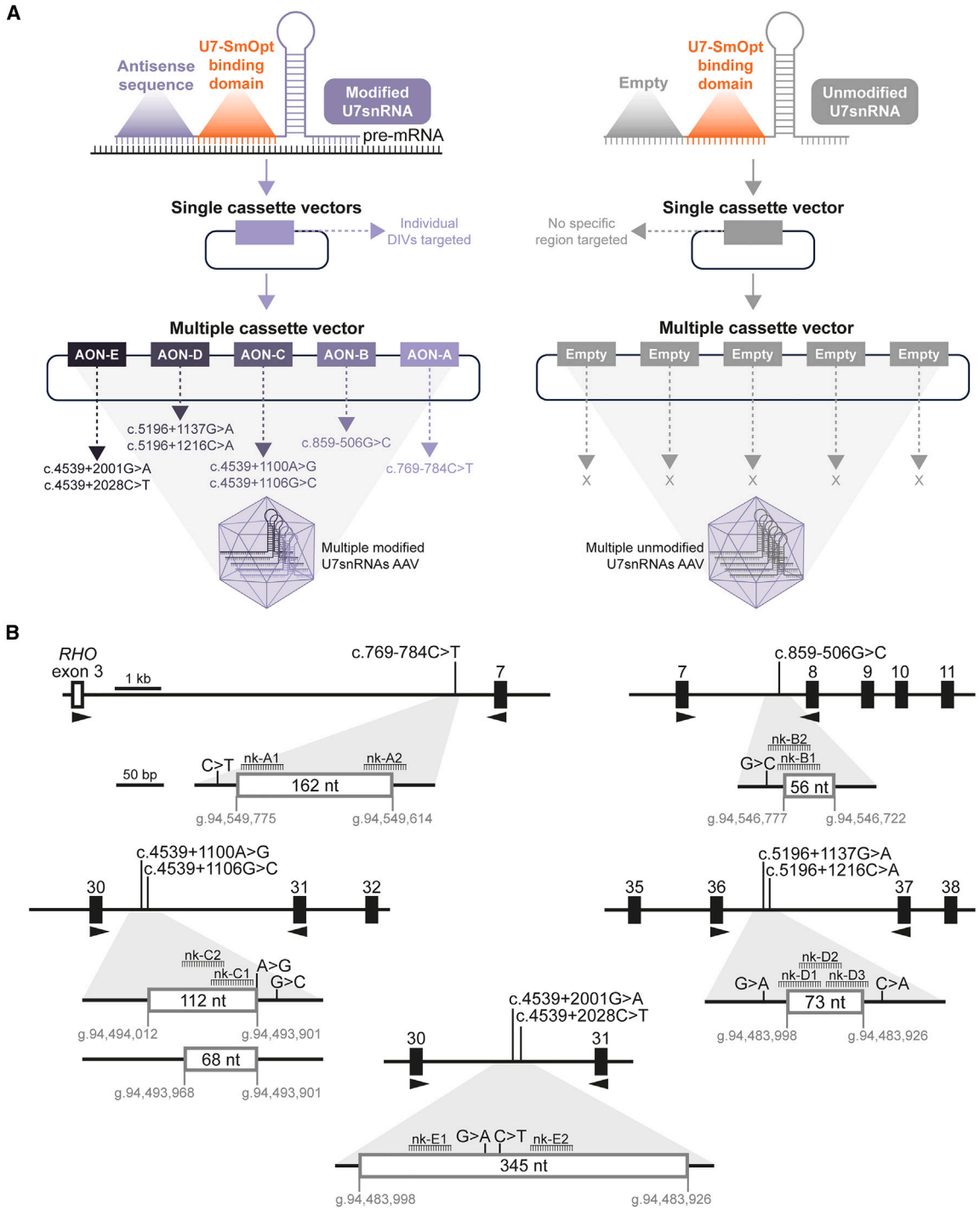

Figure 1. Experimental design used to assess U7snRNA splicing modulation capacity

(A) Schematic representation of the modified and unmodified U7snRNA vector design. Several intronic *ABCA4* variants were targeted with the single modified cassette vectors (in purple), whereas the single unmodified cassette vector (in gray) was used as a negative control for midigene-based splice assays in HEK293T. Afterward, five AON-containing U7snRNA cassettes were cloned in an individual vector to obtain the multiple modified cassette vector (in purple), a procedure that was also followed to obtain the multiple unmodified cassette vector (in gray). Both vectors were further tested in midigene-based splice assays. Then, these two multiple cassette vectors were used to derive the corresponding AAVs, which were delivered to PPCs to analyze restoration of the different splicing defects. Antisense sequences were labeled from A to E, each one targeting ≥1 intronic *ABCA4* variants as indicated by the vertical arrow below each cassette. The unmodified cassettes are also indicated as "Empty" since they do not

(legend continued on next page)

due to the rareness of each disease-causing variant, the range of required preclinical development and clinical trials for every molecular candidate is exhaustive. As an alternative strategy, previous research has shown the possibility of vectorizing these antisense sequences as a multiple delivery system that offers long-term expression in the target tissue.[26–28] The splicing modulation tool that allows this vectorization is the modified U7 small nuclear RNA (U7snRNA). Originally, the U7snRNA matures to form the U7 small nuclear ribonucleoprotein, which participates in the 3′ end processing of replication-dependent histone pre-mRNA[29] and, therefore, is not naturally involved in splicing. To improve this function and further use it as a splicing modulation tool, the wild-type (WT) Sm-binding sequence was replaced with the consensus binding sequences of Sm proteins from other spliceosomal snRNAs. In addition, the inherent histone pre-mRNA-binding sequence can also be substituted by a custom antisense sequence, allowing it to be embedded in an snRNP and protecting it from possible degradation. Collectively, this enables an Sm-optimized U7snRNA to be recruited in the nucleus by the spliceosome and to modulate the splicing of a pre-mRNA of interest.[30,31]

This study explores the potential of the U7snRNA system as a multiple-target therapy for STGD1. Accordingly, we inserted antisense sequences individually in U7snRNA cassette vectors and assessed the rescue *in vitro* of several splicing defects, after which a combination of multiple U7snRNA cassettes was inserted into a single vector and tested in both midigene-based assays and in patient-derived retinal-like cell models. This investigation provides the first extensive assessment of multiple antisense delivery for several different intronic *ABCA4* variants, which can be packaged later in an AAV to ensure prolonged expression of the U7snRNAs. Considering that these pathogenic variants are heterogeneously distributed among the STGD1 patient population, the development of a novel strategy that can target multiple variants may help to increase the number of eligible STGD1 patients for treatment and, at the same time, reduce the number of molecules needed for extensive preclinical evaluation.

RESULTS

Selection of AON sequences for U7snRNA gene modification

Several intronic *ABCA4* variants were selected to assess splicing correction by AONs delivered within a single modified U7snRNA cassette or combined as multiple cassettes within one vector (Figure 1A). Based on previous midigene-based splice assays, these variants lead to PE inclusion into the final transcript (Figure 1B) and efficacious AONs that can individually rescue these splicing defects were already identified.[11,12,15,17,25] From these earlier studies, the best-performing oligonucleotides were selected, based on their ability to prevent PE inclusion in midigene-based splice assays, and inserted into the unmodified U7snRNA gene. A total of 11 single modified U7snRNA vectors were successfully generated to target splicing defects caused by several intronic *ABCA4* variants: two for c.769-784C>T (A1 and A2), two for c.859-506G>C (B1 and B2), two for c.4539+1100A>G and c.4539+1106C>T (C1 and C2), three for c.5196+1137G>A and c.5196+1216C>A (D1, D2, and D3), and two for c.4539+2001G>A and c.4539+2028C>T (E1 and E2). In addition, a single unmodified U7snRNA vector was generated and served as a negative control in the following experiments. All single cassette vectors were validated by Sanger sequencing (Figure S1).

Single modified U7snRNA vectors specifically rescue aberrant *ABCA4* transcripts

For all intronic variants, there was a dose-response effect with increasing amounts of U7snRNA vector correlated with increased splicing correction (Figures 2 and S2), compared to each respective nontreated (NT) control. At least one of the modified U7snRNA vectors for each variant was able to restore correct transcript levels up to 60% or more of the total transcript, and in some cases, these efficacies were comparable to those shown by the respective naked AON (Figure 2A [left], 2B, 2D, and S2A–S2C). However, for some variants, such as c.769-784C>T (A2), c.4539+1106C>T (C1) and c.4539+2001G>A (E2), the efficacy of the AON was reduced when embedded in the U7snRNA molecule, compared to the corresponding naked AON sequence (Figure 2A [right], 2C, and S2B). More important, all of the tested single cassette vectors were shown to specifically target the intronic variant of interest because there were no major alterations in the observed splicing patterns of the other *ABCA4* midigenes. This was true for both WT and mutant (MT) midigene conditions where no other transcripts were created upon delivery of the different single modified U7snRNA cassettes (Figures 2 and S2).

The intronic variant c.769-784C>T is reported to cause a 162-nt PE insertion in the final transcript[12] (Figure 1B). The 2 selected AONs that target this variant (nk-A1 and nk-A2) efficiently restored the correct transcript (Figure 2A). This effect was also translated to the respective modified U7snRNA vectors, where U7snRNA-A1 and U7snRNA-A2 increased overall correct transcript levels, although this did not reach statistical significance. Interestingly, the unmodified U7snRNA vector had a clear effect on the splicing pattern, since an increase of the PE insertion levels was detected compared to the NT conditions (Figure 2A). In the case of variant c.859-506G>C, both naked AONs presented a similar rescue of the correct transcript. Again, these sequences achieved an equivalent correct transcript rescue at the highest doses when individually inserted in the U7snRNA (Figure 2B). Both variants c.4539+1100A>G and

contain an antisense sequence and are not able to specifically target a region (shown as "X"). (B) Depiction of genomic regions of all midigene constructs used in splice assays to assess efficacy of the different U7snRNA vectors, together with the splicing defects caused by each intronic variant and the relative position of the antisense sequences used in this study, sequences that are labeled as naked AON (nk) from A to E. Black boxes in midigene constructs represent the *ABCA4* exons. In the case of the c.769-784C>T midigene, RT-PCR analysis included exon 3 of *RHO*, represented as a white box because it is localized in the backbone of the splicing vector. The large size of the region between exon 6, intron 6, and exon 7 of *ABCA4* did not allow its insertion into a midigene vector. Black triangles represent the location of the primers used for the RT-PCR analyses for each midigene construct.

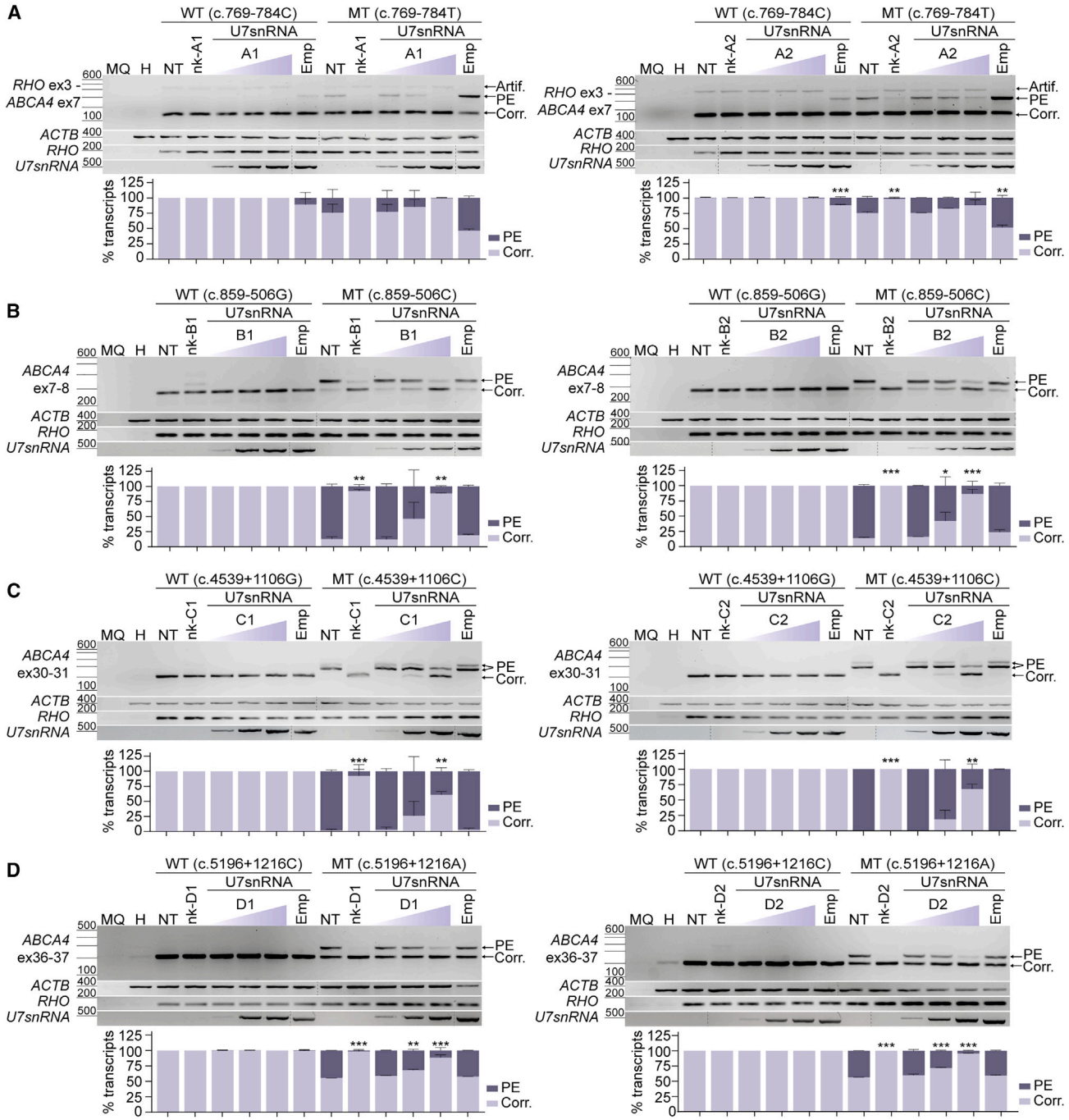

Figure 2. Splicing rescue mediated by modified single-cassette U7snRNA vectors in midigene-based splicing assays

Analysis of correct (Corr.) and pseudoexon (PE)-including *ABCA4* transcripts by RT-PCR. Wild-type (WT) midigenes and the respective mutant (MT) midigenes harboring variants c.769-784C>T (A), c.859-506G>C (B), c.4539+1106G>C (C), and c.5196+1216C>A (D) were transfected in HEK293T cells. Nontransfected cells were used as endogenous expression control (lane labeled as H). The AON-containing single-cassette U7snRNA vectors were then delivered in increasing amounts (0.035, 0.125, and 0.5 μg), except for the nontreated lanes (NT). The respective naked AONs (nk) were delivered in parallel at 0.5 μM as positive controls for splicing correction, whereas an unmodified or empty single-cassette U7snRNA vector was used as negative control (Emp). Two antisense sequences (1–2) were tested for each intronic *ABCA4* variant (A–D). RT-PCR products are shown in representative electrophoresis gel images, and the graphs below represent semiquantification of the bands of all conducted replicates, indicating the percentages of correct and PE inclusion levels in each condition. Midigene artifacts (Artif.) were not included in the analysis. MQ is used as the negative control

(legend continued on next page)

c.4539+1106C>T are reported to induce a 68-nt and a 112-nt PE insertion[12] (Figure 1B). Upon delivery of nk-C1 and nk-C2, there was a significant increase in correct transcript levels, increasing these values to more than 90% of the total transcript. In contrast, the correction efficacy of the sequences was affected after insertion in the U7snRNA cassette since the correct transcript levels were lower after U7snRNA-C1 and U7snRNA-C2 transfection for both variants compared to the nk-C1 and nk-C2 (Figures 2C and S2A).

Two other variants in intron 36 leading to the same splicing defect are c.5196+1137G>A and c.5196+1216C>A.[15] This 73-nt-long PE inclusion was completely abolished by all naked AONs (Figures 2D and S2B). Similar to previous assays, the corresponding modified U7snRNA vectors could reproduce this recovery of the correct transcript only at a higher U7snRNA amount. Despite their generally high splicing modulation efficacy, U7snRNA-D2 vector outperformed the other 2 U7snRNA vectors for both intron 36 variants, even at an intermediate transfection dose (Figures 2D and S2B). Lastly, nk-E1 and nk-E2 could successfully reduce the 345-nt PE inclusion caused by variant c.4539+2001G>A,[25] which was also the case for both U7snRNA-E1 and U7snRNA-E2 vectors (Figure S2C). To our surprise, the unmodified U7snRNA vector also showed a statistically significant decrease in aberrantly spliced transcript levels.

Collectively, these data suggest that U7snRNA-embedded AON sequences are able to efficiently rescue aberrant splicing in HEK293T cells individually, achieving similar effects when compared to the delivery of the respective naked AON molecule. Therefore, it was important to next assess whether the splicing modulation capacity and variant-targeting specificity is maintained within a combined delivery method.

Combined delivery of modified U7snRNAs maintains splicing rescue for 7 intronic *ABCA4* variants

Based on the single cassette results, the design of the multiple cassette vector included the insertion of the top five best-performing modified U7snRNA sequences (one per PE), which were U7snRNA-A1 for c.769-784C>T, U7snRNA-B2 for c.859-506G>C, U7snRNA-C2 for both c.4539+1100A>G and c.4539+1106C>T, U7snRNA-D2 for c.5196+1137G>A and c.5196+1216C>A, and U7snRNA-E1 for c.4539+2001G>A. From here on, this is described as U7snRNA-A/B/C/D/E or multiple U7snRNAs (Figure 1A). In addition to this multiple cassette vector, another one containing five unmodified (or empty) U7snRNA cassettes was generated as an additional negative control for these midigene assays. Naked AONs were used as a reference for full correction (Figures 3 and S3), and the other single U7snRNA vectors not targeting the variant of interest were considered to be an equivalent for scramble control.

Levels of aberrant transcript caused by c.769-784C>T were significantly reduced upon delivery of the nk-A, the single U7snRNA-A vector, and the multiple U7snRNAs vector (Figure 3A). Interestingly, single U7snRNA-B/C/E vectors showed a slight increase in PE inclusion band in both WT and MT midigene situations. The delivery of the unmodified empty single and multiple U7snRNA vectors, however, had a significant effect on the splicing pattern because it caused a decrease in the correct transcript levels, which was previously observed in single-cassette assays. Moreover, the midigene artifact band appeared at different intensities depending on the condition, which may have interfered with the splicing readout in this case. In contrast with these results, the correction capacity of the multiple cassette vector was similar to the nk-B and single U7snRNA-B vector for the c.859-506G>C variant, with no major changes produced by the unmodified U7snRNA vectors (Figure 3B). However, the single U7snRNA-E vector (originally targeting variant c.4539+2001G>A), had a significant rescue of the splicing defect compared to the non-treated MT condition.

The delivery of the different single modified U7snRNA or the multiple modified U7snRNA vectors did not present any adverse effects on the other analyzed *ABCA4* regions (Figures 3 and S3). For intronic variants c.4539+1100A>G and c.4539+1106G>C in intron 30, the rescue pattern was comparable between both assays since the expected treatments led to a significant decrease in the 2 PE inclusions (Figures 3C and S3A). Correct transcript levels increased to up to 70%–100% in the case of c.4539+1100A>G and c.4539+1106G>C variants when targeted with either nk-C, single U7snRNA-C, or the multiple U7snRNAs cassette vectors. Similar results were observed for intron 36 variants, where percentages of correct transcript were increased to 90%–100% upon delivery of nk-D, single U7snRNA-D, and multiple U7snRNA vectors (Figures 3D and S3B). The other single or multiple unmodified U7snRNA vectors did not alter the splicing ratios in any of these cases. Lastly, the multiple U7snRNAs vector was also able to achieve splicing modulation for variant c.4539+2001G>A, almost completely abolishing the presence of the aberrant transcript. However, a slight decrease in the 345-nt PE inclusion was observed in the case of single U7snRNA-A/B/C vectors, which was also observed after the delivery of the single or multiple unmodified U7snRNA vectors (Figure S3C). All of the observed transcripts were validated by Sanger sequencing (Figures S4 and S5).

Overall, the vector expressing all five modified U7snRNA cassettes maintained a comparable splicing rescue relative to the delivery of the respective single U7snRNA cassette vector or naked AON, although the efficacy of the AON sequences was slightly reduced for variants c.769-784C>T, c.4539+1106G>C and c.4539+2001G>A when embedded in the multiple cassette vector. Interference with splicing events was observed for variants c.769-784C>T and

of all of the reactions. Amplification of actin (*ACTB*) gene was used as loading control, exon 5 of the rhodopsin (*RHO*) gene was used as a midigene transfection control, and amplification of U7snRNA cassettes was used as vector transfection control. The dashed lines between lanes indicate the boundaries of cropped regions to facilitate data visualization; samples in the same gel image come from the same experiment replicate and RT-PCR reaction. Data (n = 2) are presented as mean ± SD. Statistical significance is indicated as *$p < 0.05$, **$p < 0.01$, and ***$p < 0.001$ using one-way ANOVA test after Dunnett's multiple comparison analysis, in which the WT or MT midigene NT column was the reference condition for correct transcript levels.

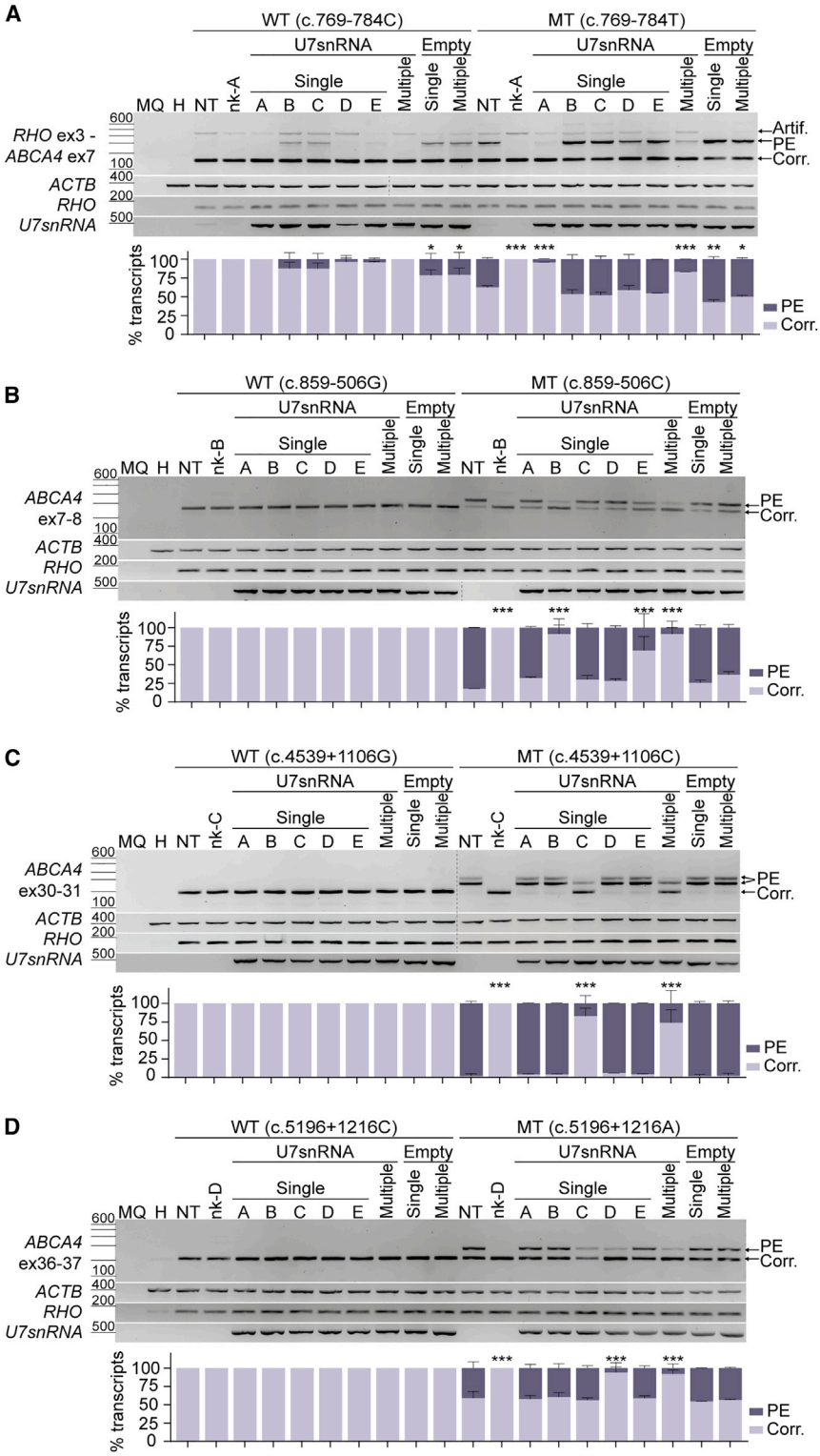

Figure 3. Splicing rescue mediated by modified multiple-cassette U7snRNA vectors in midigene-based splice assays

Analysis of correct (Corr.) and pseudoexon (PE)-including *ABCA4* transcripts by RT-PCR. Wild-type (WT) midigenes and the respective mutant (MT) midigenes harboring variants c.769-784C>T (A), c.859-506G>C (B), c.4539+1106G>C (C), and c.5196+1216C>A (D) were transfected in HEK293T cells. Nontransfected cells were used as endogenous expression control (H). The AON-containing multiple-cassette U7snRNA vector was then delivered (0.5 μg) in parallel with all 5 single-cassette vectors individually (0.5 μg), except for the nontreated lanes (NT). The respective naked AONs (nk) were delivered in parallel at 0.5 μM as positive control for splicing correction, whereas an empty single- or multiple-cassette U7snRNA vector was used as negative control. Antisense sequences targeting different splicing defects are labeled from A to E. RT-PCR products are shown in representative electrophoresis gel images, and the graphs below represent semiquantification of the bands of all of the conducted replicates, indicating the percentages of correct and PE inclusion levels in each condition. Midigene artifacts (Artif.) were not included in the analysis. MQ is used as negative control of all of the reactions. Amplification of actin (*ACTB*) gene was used as loading control, exon 5 of the rhodopsin (*RHO*) gene was used as a midigene transfection control, and amplification of U7snRNA cassettes was used as vector transfection control. The dashed lines between lanes indicate the boundaries of cropped regions to facilitate data visualization; samples in the same gel image come from the same experiment replicate and RT-PCR reaction. Data (n = 2) are presented as mean ± SD. Statistical significance is indicated as *p < 0.05, **p < 0.01, and ***p < 0.001 using the one-way ANOVA test after Dunnett's multiple comparison analysis, in which the WT or MT midigene NT column was the reference condition for correct transcript levels.

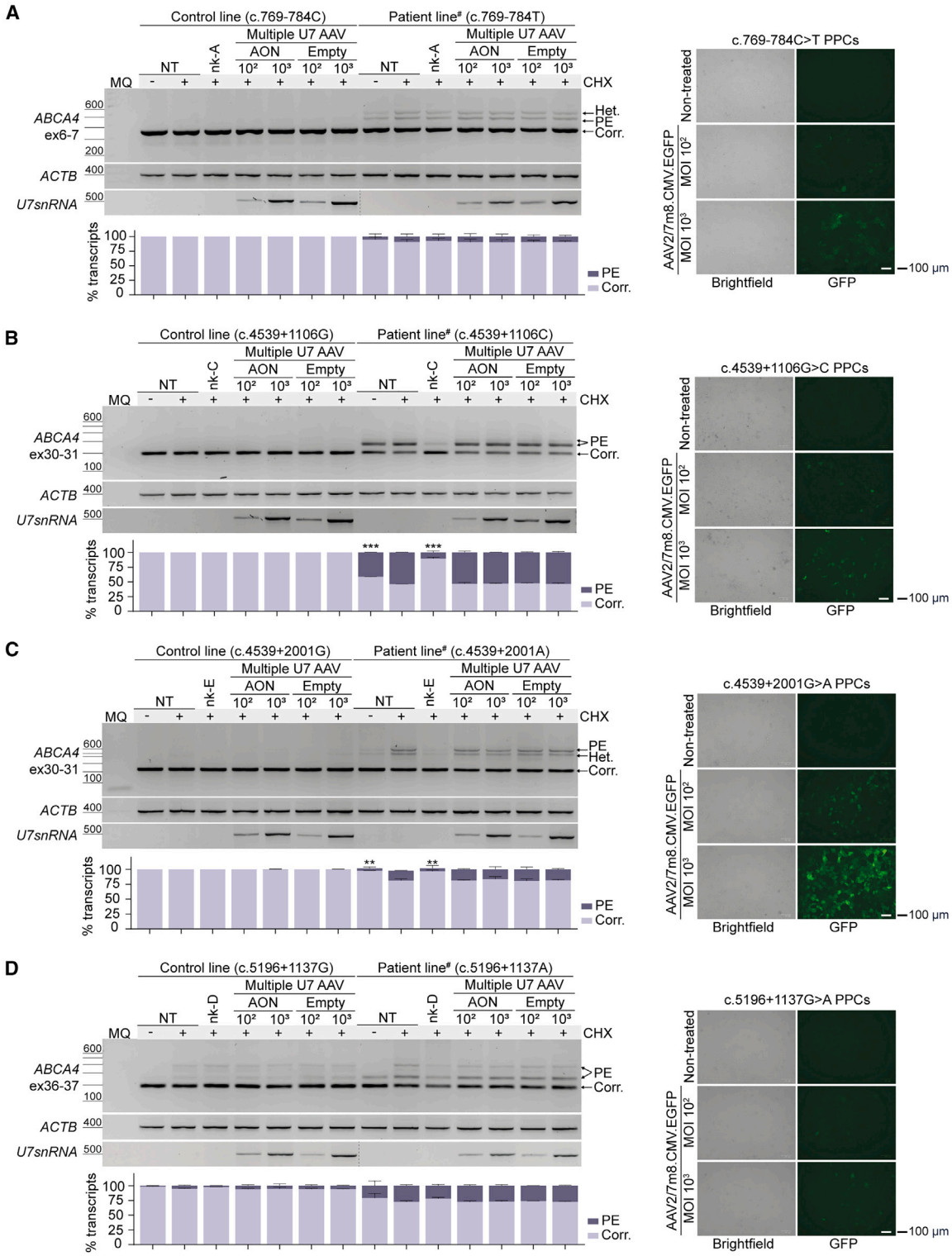

Figure 4. AAV delivery of multiple modified U7snRNAs to PPCs

Analysis of correct (Corr.) and pseudoexon (PE)-including *ABCA4* transcripts by RT-PCR (left), and assessment of AAV transduction efficiency by live fluorescence imaging (right). Control and patient individual-derived iPSCs carrying variants c.769-784C>T (A), c.4539+1106G>C (B), c.4539+2001G>A (C), and c.5196+1137G>A (D) in

(legend continued on next page)

c.4539+2001G>A, which were mainly detected after the transfection of single U7snRNA vectors targeting other regions in *ABCA4* or the unmodified U7snRNA vectors not targeting any region (Figures 2A and S3C). Despite this, the results suggest that the multiple-target approach through the simultaneous expression of several modified U7snRNAs has the potential to correct different splicing defects with a single therapeutic molecule.

Combined delivery of modified U7snRNAs to patient-derived photoreceptor precursor cells (PPCs)

As a next step, the multiple modified and unmodified U7snRNA cassette vectors were validated by Sanger sequencing and restriction analysis (Figure S6) and were used for production of the corresponding AAV particles (Figure 1A) using the AAV2/7m8 serotype, which was observed to transduce control PPCs more efficiently than other two AAV serotypes (AAV2/2 and AAV2/9; Figure S7). For transduction experiments, a control individual and six STGD1 patient-derived induced pluripotent stem cells (iPSCs) lines harboring the different intronic variants were differentiated into PPCs, which are heterogeneous 2-dimensional (2D) cultures with multiple retinal progenitor cells.[17,32] The characterization of these cultures by qRT-PCR analysis showed an increased *ABCA4* expression and a decreased pluripotency marker *OCT4* expression in all lines compared to day 0 iPSC samples (Figure S8). Higher expression of the neuroretina precursor marker *PAX6* was observed in most PPC lines, although the expression of *SIX6* was variable depending on the cell line, suggesting an early retina differentiation stage of these PPCs. The photoreceptor precursor-specific transcription factor *CRX* was kept at similar or lower levels compared to iPSCs, variability that was also observed for the S-cone opsin marker *OPN1SW* expression. The presence of RPE cell markers in these cultures was confirmed by an increase in *VMD2* expression in all differentiations.

The splicing defects observed in midigene-based assays were also detected in patient-derived PPC samples, and the transcripts were confirmed by Sanger sequencing (Figures S9 and S10). The ratios between correct and aberrant transcripts varied between the two different cell models, probably since almost all iPSC lines were heterozygous for the variant of interest. In the case of PPCs, treatment with cycloheximide (CHX) was used to inhibit aberrant transcript degradation through nonsense-mediated decay (NMD) to better represent the accumulation of the total transcript containing the corresponding PE insertion. In case of variants c.769-784C>T, c.4539+1106G>C, and c.859-506G>C, the associated splicing defect was not substantially increased by CHX treatment. In contrast, aberrant transcript accumulation was visible in cases of moderate splicing defects produced by c.4539+2001G>A, c.4539+2028C>T, and c.5196+1137G>A variants, especially after NMD inhibition (Figures 4 and S11). Upon naked AON delivery to each patient-derived PPC line, an increase in correct transcript levels was achieved for almost all of the intronic variants, except for c.859-506G>C, in which the strong PE inclusion was not rescued despite the previously high efficacy shown in midigene-based assays.

Viral transduction was done on day 25 of PPC differentiation at two different MOIs (10^2 and 10^3 viral genome [vg]/cell), using either the U7snRNA-A/B/C/D/E or multiple unmodified U7snRNAs viral vectors. Overall, the expression of the *U7snRNA* gene was detected after AAV delivery to all 7 PPC lines, suggesting a successful uptake of the viral DNA since no expression was observed in nontransduced cells. Nonetheless, the presence of the 5 different modified U7snRNA in these cells was not sufficient to achieve splicing correction, an observation that was common to all 6 patient lines (Figures 4 and S11). The only exception was a slight decrease in the 345-nt PE inclusion produced by the c.4539+2001G>A variant, which was observed after delivery of 10^3 vg/cell (from 19% to 16.5% of aberrant transcript levels compared to the CHX-treated condition) (Figure 4C). This effect, however, was not statistically significant. As expected, and in line with the expected outcomes, the AAV containing the multiple unmodified U7snRNA cassettes did not show any significant effect on splicing.

In contrast to midigene-based studies, the high correction efficacy of the multiple modified U7snRNA cassettes could not be translated into PPCs. Despite observing expression of the *U7snRNA* gene, the uptake of the viral particles by the cells of the culture was shown to be suboptimal in representative fluorescence images (Figure S12). The transduction control used in this study (AAV2/7m8.CMV.EGFP) was delivered in the same conditions as the other two customized AAVs. Increased GFP signal was observed upon AAV delivery at 10^3 vg/cell compared to 10^2 vg/cell, also shown by *U7snRNA* expression. However, variability in transduction was qualitatively noticed between the 7 PPC lines and differentiations, as well as variability of *U7snRNA* expression by RT-PCR, which may explain the low correction efficacy observed for aberrant transcripts. Moreover, to determine whether the viral genomic DNA included all 5 modified U7snRNA cassettes, we amplified several regions by PCR

heterozygosity (#), were differentiated to PPCs. Nontreated (NT) cells were used as endogenous *ABCA4* expression control. PPCs were treated (+) with cycloheximide (CHX) to assess the accumulation of total aberrant transcript produced, or were left untreated (–). AAVs harboring either the multiple AON-containing or empty U7snRNAs were delivered at 10^2 and 10^3 vg/cell, in parallel with the respective AONs (nk) at 0.5 μM as positive control for splicing correction. Antisense sequences targeting different splicing defects are labeled from A to E. RT-PCR products are shown in representative gel images, and the graphs below represent semiquantification of the bands, indicating the percentages of correct and PE inclusion levels in each condition. Heteroduplexes (Het.) were not included in the analysis. MQ is used as negative control of all of the reactions. Amplification of the actin (*ACTB*) gene was used as loading control, and amplification of U7snRNA cassettes was used as viral transduction control. The dashed lines between lanes indicate the boundaries of cropped regions to facilitate data visualization. In the case of the U7snRNA RT-PCR for the control PPC line, the same image was used to compare to patient lines (with their respective differentiation replicate) since only one line derived from a healthy individual was used for these experiments. AAV2/7m8.CMV.EGFP was used to track viral transduction qualitatively, based on GFP in PPC cultures; scale bar, 100 μm. Data (n = 2) are presented as mean ± SD. Statistical significance is indicated as $^{**}p < 0.01$ and $^{***}p < 0.001$ using one-way ANOVA test after Dunnett's multiple comparison analysis, in which CHX-treated control or patient-derived PPCs column was the reference condition for correct transcript levels.

(Figure S13A). Although all 5 modified U7snRNA cassettes were present in the total AAV stock solution, sequencing data suggested that U7snRNA-B and U7snRNA-D sequences were absent in several viral genomes (Figure S13B). This may indicate the possibility of a mixed population of AAVs of complete versus truncated genomes in multiple combinations, which was not previously detected in quality assessments of the synthesized viral preparation.

In summary, the outcome of these experiments differed from previous testing of the multiple cassette vectors in midigene-based splice assays. Therefore, the potential of the U7snRNA as a splicing correction tool could not yet be demonstrated in the context of a retinal-like cell model, although testing in the HEK293T cell model showed promising results at earlier stages of this research.

DISCUSSION

More than 2,000 different *ABCA4* variants have been discovered in STGD1 cases that are widely distributed over exonic and intronic regions in the *ABCA4* locus (www.lovd.nl/ABCA4). Intronic variants represent an important proportion of the reported disease-causing mutations and have emerged as an attractive target for genetic therapies.[5] Splicing modulation approaches are the most suitable because these variants generally cause alterations of *ABCA4* splicing at pre-mRNA levels.[21] To combat mutation specificity, in this study, we show that the simultaneous delivery of multiple AON sequences with a single therapeutic vector may efficaciously rescue the aberrant splicing caused by several intronic *ABCA4* variants, posing a novel therapeutic alternative for STGD1 by combining splicing modulation therapy with a multiple-target delivery system. The results presented in this research are an indication of the potential of this approach to rescue several splicing defects in midigene-based assays, but the translation of the observed benefits still needs to be demonstrated in retina-like models through AAV delivery.

Extensive research is ongoing for STGD1 therapeutic interventions, including molecular therapies and small compounds targeting affected metabolic pathways, cell replacement strategies, and gene-specific approaches. Within this last category, different options are under study at preclinical stages, such as gene replacement, gene editing, and splicing modulation.[18,33] For some subtypes of IRD, gene augmentation is the most advanced strategy, and this represents a suitable approach for recessive conditions such as STGD1 since it would combat disadvantages such as therapeutic design complexity, which is intrinsic to its clinical and genetic heterogeneity. However, viral vectors such as AAVs have a maximum cargo capacity of ∼4.8 kb, and the delivery of large cDNAs is therefore complicated. Some of the affected genes in IRDs, including *ABCA4*, by far exceed the size of the cDNA to be packaged. Nevertheless, AAV still represents a good choice for transgene delivery due to its tropism in the retina,[34–37] guaranteeing long-term expression upon delivery in the retina[38–40] and maintaining low immunogenicity and toxicity in the tissue.[41–44] This is also supported by the US Food and Drug Administration and the European Medicines Agency market approval for a gene therapy product (Luxturna) for a subtype of IRD due to *RPE65* variants.[45] AAV delivery also provides the opportunity to develop an alternative therapeutic approach as potential STGD1 treatments, and instead of augmenting the expression of the entire gene into retinal cells, this study proposed to implement AAV delivery of vectorized AONs to target several splicing defects.

We hypothesized that aberrant transcripts caused by the presence of intronic *ABCA4* variants are good candidates to be addressed through the U7snRNA system.[29] The small size of the corresponding gene cassette (∼410 bp) allows its packaging in AAV vectors in a single or a multiple manner, whereas the simplicity to modify the sequence offers the possibility to bind to any region of interest.[26] However, it also gives the advantage of prolonged expression in the host cell, in contrast to the transient effect of naked AONs when injected intravitreally.[46] In fact, our results show the potential of the U7snRNA to reduce the presence of several splicing defects *in vitro*, since most of the designed single cassette vectors could achieve a substantial increase in the correct transcript levels.

The use of cell lines as a first screening tool for the modified U7snRNA vectors has helped to compare the efficacy of the system to the standard naked AON delivery in a cost-effective manner. However, there are limitations to this part of the study that should be considered when interpreting the results. Note that these first comparisons in HEK293T cell line include two different types of molecules—chemically modified RNA oligonucleotide versus plasmid DNA—and it is probably the reason for lower efficacy in some modified U7snRNA vectors. In the case of the naked AON, it can modulate splicing in the nucleus after transfection of the cells, whereas all U7snRNA vectors require an intermediate step, which is gene expression before splicing modulation. This may cause a delay in observing the expected effect, which cannot be avoided by this experimental design.

Moreover, midigene-based splice assays represent the overexpression of a vector containing a genomic region of *ABCA4* in a nonretinal cell line. Therefore, the splicing readout may be influenced since the system does not fully recapitulate the genomic context nor the retinal environment of *ABCA4* splicing in the retina. This was exemplified by the assays using the midigene harboring variant c.769-784C>T, in which the presence of an artifact was already reported.[12,23] In this study, the unmodified U7snRNA vector showed significant detrimental effects when targeting this splicing defect. These events not only imply that the U7snRNA itself may interact with the splicing machinery of the cell in a nonspecific manner but also that the observed interference may be related to the midigene system itself. In addition, the PE inclusion caused by the c.4539+2001G>A variant was decreased by the unmodified U7snRNA vector, in this case resulting in a beneficial effect. These unexpected effects have been observed only when using certain midigene constructs, and were not detected in the other splice assays. It is still possible that the unmodified U7snRNAs can interfere with splicing and create these artifacts due to similarities of regions in U7snRNA with the targeted genomic regions, but the mechanisms by which it can lead to either a negative or positive effect are still unknown.

Despite these limitations, our results provide evidence for substantial splicing correction in cell line models and encourage multiple modified U7snRNAs vector testing. To our knowledge, this is the first study to examine the potential of U7snRNA system for *ABCA4* splicing modulation in STGD1. When testing the multiple cassette vector *in vitro*, the efficacy was maintained for all of the tested intronic variants compared to the single approach. Furthermore, the efficiency for the multiple U7snRNA delivery may be a synergistic outcome, since the observed results represent the combined contribution of all of the individual cassettes. These findings are similar to those reported in studies conducted in Duchenne muscular dystrophy for multiexon skipping, in which the removal of the affected exons of the dystrophin transcript was successfully achieved in a mouse model, confirming the potential of this splicing modulation tool to reduce aberrant transcripts *in vivo*.[26,28]

Unfortunately, the translation of these results to patient-derived PPCs was not possible in this study (Figures 4 and S11). Although expression of *U7snRNA* was detected only in the transduced cells by RT-PCR analysis, an uneven distribution of the transduction control AAV was observed in these cell differentiations. Surprisingly, this variability was extended to most of the differentiations, as shown by the fluorescence images from representative parallel cultures (Figure S12). In previous research, the AAV2/7m8 serotype expressing GFP was demonstrated to have the best tropism among other tested serotypes in human iPSCs, RPE cells, and cortical neurons.[35] However, the tested dosages were between 10 and 1,000 times higher than the ones used in our assays, and the AAV exposure time was shorter for iPSC, RPE cells, and cortical neurons (in this case, prolonged up to 96 h). Higher doses and longer exposures were previously attempted in mouse retina, retina-on-chip models,[47] and human iPSC-derived retinal organoids,[48] in which a correlation between the uptake of viral particles and the presence of the required cell surface ligands for AAV2/7m8 entry into the host cells was found. These markers are part of the heparan sulfate proteoglycan family and are reported to have an important role in neuroretinal development.[49,50] Considering that the expression of these cell surface proteoglycans was already detected in photoreceptor precursor cells from early retinal organoids (differentiated for 44 and 70 days), the AAV2/7m8 serotype still serves as a good option for both early or more mature retinal-like cell models.

Since the goal of this research was to develop a novel therapeutic approach, lower MOIs and more prolonged exposure times were selected considering the toxicity and immunogenicity issues that may arise in the future if higher doses of the viral vector are used. For that reason, further optimization of the experimental design should be focused on the time course rather than increasing the amount of virus delivered. However, the window for treatment remains relatively limited in the 30-day differentiation protocol into PPCs, comparing it to longer 3D differentiation cultures.[51] More important, dose-dependent immune responses have been reported in previous clinical trials, in which inflammation was detected in those patients treated subretinally with higher AAV2 doses.[52–55] Despite the ocular immune privilege,[56,57] activation of innate immune responses by both the single-stranded DNA genome and the capsid proteins of AAV2 and 8 serotypes have been detected in the retina and other tissues, which was suggested to explain the reduced transduction efficiency observed in previous research.[41,43,58] However, modifying motifs in the viral genome seems to be a promising alternative to avoid innate recognition and could be used in combination with additional immunomodulation strategies.[59] In the case of the AAV2/7m8 serotype used in this study, capsid-associated immunotoxicity issues have not been reported yet.

The low efficacy of the multiple modified U7snRNA cassette in rescuing splicing could also be improved by modifying the sequences vectorized in this system. The fact that a naked chemically modified AON rescues a splicing defect up to 100% does not guarantee its efficacy when embedded in the U7snRNA; therefore, this could be an aspect to further study and test to achieve better performance of the multiple sequence delivery. For instance, it may be possible to insert longer antisense sequences as performed in previous studies, in which those AAVs were able to rescue *CEP290* aberrant splicing more efficaciously than the ones delivering shorter sequences.[28] Although these characteristics can be improved, it does not completely explain the lack of an effect in our patient-derived PPC assays.

It is also important to mention that some of the nk-AONs (nk-A, nk-B, and nk-D) used as a control for splicing correction also presented minimal rescue on PPC assays, whereas in midigene assays, the nk-AONs showed full rescue in most of the cases. This suggests that the rescue of shorter *ABCA4* transcripts produced by the midigene construct may be more efficient than the rescue of endogenous *ABCA4* transcripts in PPCs, perhaps due to differences in secondary structures that make the endogenous transcript less accessible also for the nk-AONs. Nonetheless, the fact that nk-C and nk-E were able to significantly rescue aberrant splicing in PPCs indicates that the AAV uptake is more likely to be the limiting factor rather than the accessibility of these *ABCA4* regions (Figures 4 and S11).

An unexpected finding that may contribute, in part, to the observed outcome is the deletion of some modified U7snRNA gene cassettes detected in the sequencing of the viral DNA (Figure S13). It is known that challenges in AAV manufacturing, such as filtration, purification, empty capsid separation, product degradation, and physical instability, among others, can affect outcomes.[60] Taking into account that the original plasmid was previously checked and contained all cassettes (Figure S6), this event may indicate that potential recombination between the U7snRNA sequences could have occurred at the viral production level. In fact, previous research on AAV-genome population sequencing on Cas9-single guide RNA vectors has shown that self-complementary sequences in the viral vector design, together with DNA secondary structures of the transgene or the inverted terminal repeat (ITR) heterogeneity, can cause truncated versions of vector genomes, which can have a negative impact on AAV production and efficacy.[61]

In conclusion, the low transduction efficiency observed in our cell model, together with a reduced number of AAV particles containing

the full cargo, could be impeding the splicing modulation capacity of the multiple-delivery system designed in this study. For that reason, more research will be required to refine and overcome the AAV synthesis challenges that were encountered here, an issue that will have to be considered during quality assessments for those cargos that are designed to become a combined therapeutic approach. Our research attempted to develop an approach that combines the specificity of splicing modulation strategy and the efficacy of viral vector delivery, but this will require optimization of the step between from plasmid DNA to viral vector. Therefore, the feasibility of implementing the multiple modified U7snRNA in a single delivery method as a potential treatment for a larger IRD patient population, still remains uncertain.

MATERIALS AND METHODS

U7snRNA constructs design

AON sequences targeting splicing defects caused by variants c.769-784C>T, c.859-506G>C, c.4539+1100A>G, c.4539+1106C>T, c.4539+2001G>A, c.4539+2028C>T, c.5196+1137G>A, and c.5196+1216C>A were selected from previous screenings in midigene-based splice assays.[11,12,15,17,25] These sequences (Table S1) were inserted into the unmodified or empty U7snRNA gene and then cloned into a pSMD2 shuttle vector (kindly provided by Dr. Aurélie Goyenvalle).[27] For the single U7snRNA cassette vectors, each AON sequence was inserted individually through a two-step PCR approach, as previously described.[62] For PCR-I, the used forward primer contained the XbaI restriction site and the 5′ region of the U7snRNA gene (Fw-U7-XbaI), whereas part of the antisense sequence to be inserted was included in the reverse primer. In parallel, PCR-II was performed using a forward primer with the part of the antisense sequence and a reverse primer containing NheI restriction site and the 3′ region of the U7snRNA gene (Rv-U7-NheI). Products from PCR-I and PCR-II were run in a 2% (w/v) agarose gel, and DNA was extracted with nucleospin gel and the PCR Clean-up Mini Kit (Macherey-Nagel Düren, Nordrhein-Westfalen, Germany) as indicated in the manufacturer's instructions. Afterward, PCR-III was performed with both extracted products and Fw-U7-XbaI/Rv-U7-NheI primers. The PCR mixtures (50 μL) contained 0.5 μM of each primer (all listed in Table S2), 0.2 mM deoxyribonucleotide triphosphates (dNTPs), 1 U Phusion High-Fidelity DNA Polymerase (New England Biolabs, Leiden, the Netherlands), 1× Phusion High-Fidelity Buffer, 0.5× Q-solution (Qiagen, Venlo, the Netherlands), and 25 ng of unmodified U7snRNA pSMD2 vector for PCR-I and -II or 1 μL of extracted products for PCR-III as templates. PCR conditions were the following: initial denaturation at 98°C for 30 s, 30 cycles at 98°C for 10 s, annealing at 58°C for 30 s, and extension at 72°C for 30 s, with a final extension at 72°C for 10 min. PCR-III products were resolved in 2% agarose gel and extracted, then incubated with XbaI and NheI (New England Biolabs) for 3 h at 37°C, followed by heat inactivation at 65°C for 20 min, to digest the modified U7snRNA gene cassette. Digestion of 1 μg of the empty pSMD2 vector was performed for 3 h at 37°C with XbaI, followed by heat inactivation at 65°C for 20 min and incubation with USB Shrimp Alkaline Phosphatase (Affymetrix, Cleveland, OH, USA) for 1 h at 37°C. The digested plasmid was resolved in 1% agarose gel, and the band of interest was extracted as previously indicated. Ligation of the digested PCR-III product and pSMD2 vector was done with a molar ratio 1:6 (vector:insert) by using T4 ligase kit (New England Biolabs) as indicated in the manufacturer's instructions. Subsequently, 5 μL of the digestion was transformed in DH5α-competent *Escherichia coli* (Life Technologies, Bleiswijk, the Netherlands). Upon picking colonies and plasmid isolation, the insertion of the modified U7snRNA cassette was validated by restriction analysis and further Sanger sequencing (Figure S1).

In the case of multiple U7snRNA cassette vectors, one initial single modified U7snRNA-A vector and the next modified U7snRNA cassette to be inserted (PCR-III product) were digested and ligated, as previously indicated. Subsequently, 5 μL of the digestion was transformed in One Shot Stbl3 Chemically Competent *E. coli* (Life Technologies). Upon picking colonies and plasmid isolation, the insertion of a second modified U7snRNA cassette was validated by restriction analysis and Sanger sequencing. This process was performed sequentially for all of the cassettes until obtaining a final pSMD2 shuttle vector containing 5 different modified U7snRNA cassettes, and in parallel, the same procedure was followed to add up to 5 unmodified U7snRNA cassettes as shown in Figure 1A.

Single and multiple modified U7snRNAs studies in HEK293T cells

HEK293T (American Type Culture Collection no. CRL-3216) cells were cultured in DMEM supplemented with 10% fetal bovine serum, 1% penicillin-streptomycin, and 1% sodium pyruvate at 37°C and 5% CO_2. To validate the efficacy of the modified U7snRNA vectors, HEK293T cells were seeded in 6-well plates in 70% confluency (∼400,000 cells per well). Four hours post-seeding, cells were left non-transfected (as endogenous control) or transfected with either the WT or the MT *ABCA4* midigene harboring the genomic region of interest (600 ng). The WT and MT midigenes that were used were obtained from previous research.[10] After overnight incubation, each midigene-transfected well was subdivided in as many wells of a 24-well plate as conditions tested. In single-cassette assays, cells were subsequently transfected with naked AON (0.5 μM) as positive control for splicing correction, three increasing amounts of the respective modified single U7snRNA vector (0.035, 0.125 and 0.5 μg), the unmodified single U7snRNA vector (0.5 μg) as negative control, or left nontreated (NT). In multiple cassette assays, the NT and positive controls were done as indicated above, cells were transfected with the 5 single modified U7snRNA vectors (0.5 μg) separately, the multiple modified U7snRNAs vector (0.5 μg), the single unmodified U7snRNA vector, and multiple unmodified U7snRNAs vector (0.5 μg) as negative controls. Midigene and U7snRNA vector transfections were performed by following the FuGENE HD (Promega, Madison, WI, USA) reagent's protocol (ratio vector:FuGENE of 1:3). Naked AONs were resuspended at 100 μM in autoclaved 1× PBS, and delivery was made as previously described elsewhere.[63] The oligonucleotides were purchased from Eurogentec (Liege, Belgium) and had phosphorothioate backbone and 2′-*O*-methyl (2′-OMe) sugar modification in all of the nucleotides. After 48 h, cells were harvested in PBS for subsequent RNA analysis. The

above-mentioned splice assays were performed in 2 independent replicates (n = 2).

Viral vector synthesis and gDNA sequencing

Two different AAV2/7m8 were synthesized for further PPC studies, one containing the 5 modified U7snRNA cassettes and another one containing 5 unmodified U7snRNA cassettes derived from the tested pSMD2 shuttle vectors. Plasmid DNA was purified by using the EndoFree Plasmid Mega kit (Qiagen) and the insert was then validated with Sanger sequencing (Figure S6A; Table S3). The integrity of the ITRs flanking the insert of interest was also checked by restriction analysis (Figure S6B). Afterwards, the modified and unmodified U7snRNA vectors were used for further customized viral synthesis (service purchased from the Gene Transfer Vector Core [https://www.vdb-lab.org/vector-core/] at Massachusetts Eye and Ear of Boston). To validate the genomic DNA (gDNA) sequence of the AAV vector containing the modified U7snRNA cassettes, Amplification Grade DNase I (Thermo Fisher Scientific, Waltham, MA) incubation was performed for 30 min at 37°C. PCR mixtures (50 μL) contained 0.5 μM of each primer (all listed in Table S4), 0.2 mM dNTPs, 1 U Phusion High-Fidelity DNA Polymerase (New England Biolabs, Leiden, the Netherlands), 1× Phusion High-Fidelity Buffer, 0.5× Q-solution (Qiagen), and 3 μL of DNase-treated AAV as template. PCR conditions were the following: initial denaturation at 98°C for 30 s, 30 cycles at 98°C for 10 s, annealing 58°C for 30 s, and extension at 72°C for 30 s, with a final extension at 72°C for 10 min. PCR products were resolved in 2% agarose gel and extracted as previously indicated. Bands were cloned with pGEM-T Easy Vector System kit (Promega) and further validated by Sanger sequencing (Figure S13).

The study was conducted in accordance with the Declaration of Helsinki, and approved by CMO regio Arnhem-Nijmegen and local Radboudumc ethics committee (CMO-light), protocol number 2015–1543.

Patient-derived iPSC culture conditions and differentiation to PPCs

Control and patient iPSCs were reprogrammed from fibroblasts or blood samples as previously described[15,17,25,64] and characterized by the Stem Cell Technology Center (Radboudumc, Nijmegen, the Netherlands). The splicing defects and intronic *ABCA4* variants were selected according to the availability of the corresponding patient-derived iPSC lines in the department and previously identified successful AON sequences. Material derived from patients harboring variants c.4539+1100A>G and c.5196+1216C>A was unavailable. The line carrying the c.4539+2028C>T variant was later included for AAV delivery assays since the associated splicing defect is not visible in midigene vectors. The patient-derived iPSC line harboring the variant c.4539+1106G>C was obtained and characterized by De Baere's research group (data not shown). iPSCs were cultured at 37°C and 5% CO_2 in Essential 8 Flex Medium (Gibco, Dallas, TX, USA) supplemented with 100 μg/mL Primocin (InvivoGen, Toulouse, France). The maintenance of iPSC lines was done on 6-well plates coated with GelTrex (Gibco) at 240–360 μg/mL final concentration. To derive PPCs from iPSCs, a 31-day 2D differentiation protocol was adapted from previous studies.[65,66] Single-cell seeding was performed by dissociating iPSC culture with TrypLE Express solution (Gibco) and counted. A total of 10^6 cells per well were seeded with RevitaCell Supplement (Gibco) on 12-well plates previously coated with Matrigel Growth Factor Reduced Basement Membrane Matrix at a 1:20 dilution (Corning, Corning, NY, USA). iPSCs were then cultured with Essential 8 Flex Medium until reaching full confluency. Once achieved, it was replaced by COCO/insulin-like growth factor (IGF)-based differentiation medium (CI), which consisted of DMEM:Nutrient Mixture F-12 medium (Merck, Darmstadt, Germany) supplemented with MEM nonessential amino acid solution (Sigma-Aldrich, St. Louis, MO, USA), B-27 supplement (without vitamin A, Thermo Fisher Scientific), N-2 supplement (Thermo Fisher Scientific), 100 ng/μL IGF-1 (Sigma-Aldrich), 10 ng/μL of recombinant human basic fibroblast growth factor (Sigma-Aldrich), 10 μg/μL of heparin (Sigma-Aldrich), 200 μg/mL of recombinant human COCO protein (R&D Systems, Minneapolis, MN), and 100 μg/mL Primocin (InvivoGen). Half of the medium was replaced on a daily basis to each well for 31 days.

Delivery of AAV vectors and AONs in PPCs

On day 25 of differentiation, the AAVs (modified or unmodified U7snRNA multiple-cassette AAVs and AAV2/7m8.CMV.EGFP as transduction control) were delivered at an MOI of 10^2–10^3 vg/cell in 0.5 mL of CI medium, based on the number of total cells. This was followed by medium addition up to 1 mL on day 26 and complete medium replacement on day 27. However, PPCs were treated with AON at 0.5 μM on day 29. AONs were first mixed with CI medium and were gymnotically delivered to the corresponding wells. On day 30, CHX was added to the medium at 100 μg/mL final concentration, and one of the wells for each cell line was kept as nontreated (NT). Twenty-four hours later, cells were washed with PBS and harvested in lysis buffer for further RNA analysis. Transduction levels in PPCs were qualitatively analyzed with ZOE Fluorescent Cell Imager (Bio-Rad, Lunteren, the Netherlands) in 20× magnification before harvesting. All of the differentiation experiments were performed in two independent biological duplicates (n = 2).

RNA isolation and cDNA synthesis

RNA was isolated from HEK293T cells and PPCs using the Nucleospin RNA kit (Macherey-Nagel Düren) as indicated in the manufacturer's instructions. For cDNA synthesis from HEK293T samples, 1 μg of total RNA was used as the initial input for the reaction, which was performed with the iScript cDNA Synthesis kit (Bio-Rad) to a final concentration of 50 ng/μL. For PPCs, RNA was first precipitated with ethanol as indicated in previous protocols.[67] For cDNA synthesis, 1 μg of total RNA was used for all of the reactions using the SuperScript VILO Master Mix (Thermo Fisher Scientific) and following the manufacturer's instructions.

PPC characterization by qPCR

RNA from either the corresponding iPSC (day 0) or PPC (day 31) lines was isolated as described above, and 1 μg of total RNA was

used for cDNA synthesis with the SuperScript VILO Master Mix (Thermo Fisher Scientific), as indicated above. qPCR reactions were prepared with the GoTaq Real-Time Quantitative PCR Master kit (Promega) and performed in the Applied Biosystem QuantStudio 5 Digital system. Expression levels of 7 PPC markers and one housekeeping gene (*GUSB*) were analyzed to characterize the differentiation to PPCs of the 7 iPSC lines. The primer list for qPCR markers is included in Table S5. Expression of the *GUSB* housekeeping gene was used to normalize each sample, and relative expression levels from each marker in PPCs (day 31) was compared to the respective iPSCs (day 0) using the $2^{-\Delta\Delta Ct}$ method.[68]

RT-PCR analysis for *ABCA4* transcripts

For HEK293T assays, all of the reaction mixtures (25 μL) contained 10 μM of each primer pair, 2 mM of dNTPs, 1.5 mM $MgCl_2$, 0.5× Q-solution (Qiagen), 1 U of Taq polymerase (Roche, Penzberg, Germany), and 60 ng of input cDNA. PCR conditions were 94°C for 30 s, followed by 35 cycles of 30 s at 94°C, 30 s at 58°C, and 1 min at 72°C, with a final extension step of 10 min at 72°C. For patient-derived PPC assays, all of the reaction mixtures (25 μL) contained 10 μM of each primer pair (all listed in Table S6), 2 mM of dNTPs, 1.5 mM $MgCl_2$, 0.5× Q-solution (Qiagen), 1 U of Taq polymerase (Roche), and 50 ng of input cDNA. PCR conditions were 94°C for 2 min, followed by 35 cycles of 30 s at 94°C, 30 s at 58°C, and 70 s at 72°C, with a final extension step of 2 min at 72°C. Exons 3–4 of *ACTB* were used as a loading control, exon 5 of *RHO* was used as a midigene transfection control, and *U7snRNA* was used as a transfection control for U7snRNA vectors or as a transduction control for U7snRNA AAVs. All of the PCR products were resolved on 2% agarose gels and the transcripts were analyzed by Sanger sequencing. Transcript ratios were analyzed by the semiquantification of PCR products with Fiji software,[69] based on the percentage of correct or PE inclusion transcripts in each condition or lane (Tables S7–S9).

Statistical analysis

Data were expressed as means ± SDs and processed with GraphPad Prism 9 software. To analyze the differences between the tested conditions, we used the one-way ANOVA test followed by Dunnett's multiple comparison analysis, using the NT or the CHX-treated column as reference for the correct transcript levels for HEK293T or PPC studies, respectively. Statistical significance was determined for p values smaller than 0.05, presented with one or multiple asterisks (*) in the figures depending on the significance.

DATA AND CODE AVAILABILITY

The data supporting the findings of this research are available within the article and supplemental information. Raw data are available upon reasonable request from the corresponding author.

SUPPLEMENTAL INFORMATION

Supplemental information can be found online at https://doi.org/10.1016/j.ymthe.2024.01.019.

ACKNOWLEDGMENTS

We thank all of the patients for donating the cells and taking part in this study in the search for new therapeutic approaches. We acknowledge Ymkje Hettinga, Carel B. Hoyng, Nathalie M. Bax, Rando Allikmets, and Sarah Naessens for kindly providing the patient-derived material used for further reprogramming, as well as the Radboud University Stem Cell Technology Centre for the iPSC reprogramming from healthy individual and patient-derived material. We also thank Saskia van der Velde-Visser for cell culture technical assistance. We acknowledge the Gene Transfer Vector Core at Massachusetts Eye and Ear in Boston for their assistance in evaluating the customized AAV vectors' integrity and troubleshooting. We are also grateful to Dr. Aurélie Goyenvalle for contributing to helpful discussions and feedback, as well as to Prof. Frans P.M. Cremers' research group for all of the engineered *ABCA4* midigene constructs used in this study. This research was financially supported by the European Union's Horizon 2020 research and innovation program Marie Skłodowska-Curie Innovative Training Network (ITN) StarT, with grant no. 813490 (to R.W.J.C. and M.E.C), the Foundation Fighting Blindness USA Project Program Award (PPA-0517–0717-RAD to R.W.J.C and A.G.), the Translational Research Acceleration Program of the Foundation Fighting Blindness USA (TA-GT-0521-0799-RAD-TRAP, to R.W.J.C.), The Wellcome Trust (205041, to M.E.C.) and Fight for Sight (5053/50584, to M.E.C.). The funding organizations provided unrestricted grants and had no role in the design or conduct of this research.

AUTHOR CONTRIBUTIONS

Conceptualization, A.G. and R.W.J.C. Investigation, N.S.-H., I.B.R., L.D., I.V.-D., D.W.K., and D.P. Validation, N.S.-H. Formal analysis, N.S.-H. and I.B.R. Visualization, N.S.-H. Writing – original draft, N.S.-H. Writing – review & editing, N.S.-H., I.B.R., L.D., I.V.-D., D.W.K., D.P., M.B., E.D.B., M.E.C., A.G., and R.W.J.C. Resources, M.B. and E.D.B. Project administration, N.S.-H., A.G., and R.W.J.C. Supervision, M.E.C., A.G., and R.W.J.C. Funding acquisition, M.E.C., A.G., and R.W.J.C. All of the authors have read and agreed to the final version of the manuscript.

DECLARATION OF INTERESTS

R.W.J.C. is Chief Scientific Officer of Astherna B.V. I.V.D. has been employed by Astherna B.V. since April 2023, and her contribution to this manuscript was performed before her appointment. R.W.J.C. and A.G. are listed as inventors on several filed patents for antisense oligonucleotides (WO2013036105A1, WO2018109011A1, WO2020015959A1, WO2020115106A1, and WO2021023863A1). The remainder of the authors declare no competing interests.

REFERENCES

1. Georgiou, M., Fujinami, K., and Michaelides, M. (2021). Inherited retinal diseases: Therapeutics, clinical trials and end points-A review. Clin. Exp. Ophthalmol. *49*, 270–288.

2. Bujakowska, K.M., Liu, Q., and Pierce, E.A. (2017). Photoreceptor Cilia and Retinal Ciliopathies. Cold Spring Harb. Perspect. Biol. *9*, a028274.

3. Dockery, A., Stephenson, K., Keegan, D., Wynne, N., Silvestri, G., Humphries, P., Kenna, P.F., Carrigan, M., and Farrar, G.J. (2017). Target 5000: Target Capture Sequencing for Inherited Retinal Degenerations. Genes (Basel) *8*, 304.
4. Tanna, P., Strauss, R.W., Fujinami, K., and Michaelides, M. (2017). Stargardt disease: clinical features, molecular genetics, animal models and therapeutic options. Br. J. Ophthalmol. *101*, 25–30.
5. Cremers, F.P.M., Lee, W., Collin, R.W.J., and Allikmets, R. (2020). Clinical spectrum, genetic complexity and therapeutic approaches for retinal disease caused by ABCA4 mutations. Prog. Retin. Eye Res. *79*, 100861.
6. Tsybovsky, Y., Molday, R.S., and Palczewski, K. (2010). The ATP-binding cassette transporter ABCA4: structural and functional properties and role in retinal disease. Adv. Exp. Med. Biol. *703*, 105–125.
7. Molday, R.S. (2015). Insights into the Molecular Properties of ABCA4 and Its Role in the Visual Cycle and Stargardt Disease. Prog. Mol. Biol. Transl. Sci. *134*, 415–431.
8. Zernant, J., Xie, Y.A., Ayuso, C., Riveiro-Alvarez, R., Lopez-Martinez, M.A., Simonelli, F., Testa, F., Gorin, M.B., Strom, S.P., Bertelsen, M., et al. (2014). Analysis of the ABCA4 genomic locus in Stargardt disease. Hum. Mol. Genet. *23*, 6797–6806.
9. Carss, K.J., Arno, G., Erwood, M., Stephens, J., Sanchis-Juan, A., Hull, S., Megy, K., Grozeva, D., Dewhurst, E., Malka, S., et al. (2017). Comprehensive Rare Variant Analysis via Whole-Genome Sequencing to Determine the Molecular Pathology of Inherited Retinal Disease. Am. J. Hum. Genet. *100*, 75–90.
10. Sangermano, R., Khan, M., Cornelis, S.S., Richelle, V., Albert, S., Garanto, A., Elmelik, D., Qamar, R., Lugtenberg, D., van den Born, L.I., et al. (2018). ABCA4 midigenes reveal the full splice spectrum of all reported noncanonical splice site variants in Stargardt disease. Genome Res. *28*, 100–110.
11. Bauwens, M., Garanto, A., Sangermano, R., Naessens, S., Weisschuh, N., De Zaeytijd, J., Khan, M., Sadler, F., Balikova, I., Van Cauwenbergh, C., et al. (2019). ABCA4-associated disease as a model for missing heritability in autosomal recessive disorders: novel noncoding splice, cis-regulatory, structural, and recurrent hypomorphic variants. Genet. Med. *21*, 1761–1771.
12. Sangermano, R., Garanto, A., Khan, M., Runhart, E.H., Bauwens, M., Bax, N.M., van den Born, L.I., Khan, M.I., Cornelis, S.S., Verheij, J.B.G.M., et al. (2019). Deep-intronic ABCA4 variants explain missing heritability in Stargardt disease and allow correction of splice defects by antisense oligonucleotides. Genet. Med. *21*, 1751–1760.
13. Fadaie, Z., Khan, M., Del Pozo-Valero, M., Cornelis, S.S., Ayuso, C., Cremers, F.P.M., Roosing, S., and The Abca Study, G. (2019). Identification of splice defects due to noncanonical splice site or deep-intronic variants in ABCA4. Hum. Mutat. *40*, 2365–2376.
14. Khan, M., Cornelis, S.S., Pozo-Valero, M.D., Whelan, L., Runhart, E.H., Mishra, K., Bults, F., AlSwaiti, Y., AlTalbishi, A., De Baere, E., et al. (2020). Resolving the dark matter of ABCA4 for 1054 Stargardt disease probands through integrated genomics and transcriptomics. Genet. Med. *22*, 1235–1246.
15. Khan, M., Arno, G., Fakin, A., Parfitt, D.A., Dhooge, P.P.A., Albert, S., Bax, N.M., Duijkers, L., Niblock, M., Hau, K.L., et al. (2020). Detailed Phenotyping and Therapeutic Strategies for Intronic ABCA4 Variants in Stargardt Disease. Mol. Ther. Nucleic Acids *21*, 412–427.
16. Del Pozo-Valero, M., Riveiro-Alvarez, R., Martin-Merida, I., Blanco-Kelly, F., Swafiri, S., Lorda-Sanchez, I., Trujillo-Tiebas, M.J., Carreño, E., Jimenez-Rolando, B., Garcia-Sandoval, B., et al. (2022). Impact of Next Generation Sequencing in Unraveling the Genetics of 1036 Spanish Families With Inherited Macular Dystrophies. Invest. Ophthalmol. Vis. Sci. *63*, 11.
17. Albert, S., Garanto, A., Sangermano, R., Khan, M., Bax, N.M., Hoyng, C.B., Zernant, J., Lee, W., Allikmets, R., Collin, R.W.J., and Cremers, F.P.M. (2018). Identification and Rescue of Splice Defects Caused by Two Neighboring Deep-Intronic ABCA4 Mutations Underlying Stargardt Disease. Am. J. Hum. Genet. *102*, 517–527.
18. Vázquez-Domínguez, I., Garanto, A., and Collin, R.W.J. (2019). Molecular Therapies for Inherited Retinal Diseases-Current Standing, Opportunities and Challenges. Genes (Basel) *10*, 654.
19. Collin, R.W.J., and Garanto, A. (2017). Applications of antisense oligonucleotides for the treatment of inherited retinal diseases. Curr. Opin. Ophthalmol. *28*, 260–266.
20. Havens, M.A., and Hastings, M.L. (2016). Splice-switching antisense oligonucleotides as therapeutic drugs. Nucleic Acids Res. *44*, 6549–6563.
21. Hammond, S.M., and Wood, M.J.A. (2011). Genetic therapies for RNA mis-splicing diseases. Trends Genet. *27*, 196–205.
22. Hammond, S.M., Aartsma-Rus, A., Alves, S., Borgos, S.E., Buijsen, R.A.M., Collin, R.W.J., Covello, G., Denti, M.A., Desviat, L.R., Echevarría, L., et al. (2021). Delivery of oligonucleotide-based therapeutics: challenges and opportunities. EMBO Mol. Med. *13*, e13243.
23. Tomkiewicz, T.Z., Nieuwenhuis, S.E., Cremers, F.P.M., Garanto, A., and Collin, R.W.J. (2022). Correction of the Splicing Defect Caused by a Recurrent Variant in ABCA4 (c.769-784C>T) That Underlies Stargardt Disease. Cells *11*.
24. Tomkiewicz, T.Z., Suárez-Herrera, N., Cremers, F.P.M., Collin, R.W.J., and Garanto, A. (2021). Antisense Oligonucleotide-Based Rescue of Aberrant Splicing Defects Caused by 15 Pathogenic Variants in ABCA4. Int. J. Mol. Sci. *22*, 4621.
25. Garanto, A., Duijkers, L., Tomkiewicz, T.Z., and Collin, R.W.J. (2019). Antisense Oligonucleotide Screening to Optimize the Rescue of the Splicing Defect Caused by the Recurrent Deep-Intronic ABCA4 Variant c.4539+2001G>A in Stargardt Disease. Genes (Basel) *10*, 452.
26. Goyenvalle, A., Wright, J., Babbs, A., Wilkins, V., Garcia, L., and Davies, K.E. (2012). Engineering multiple U7snRNA constructs to induce single and multiexon-skipping for Duchenne muscular dystrophy. Mol. Ther. *20*, 1212–1221.
27. Goyenvalle, A. (2012). Engineering U7snRNA Gene to Reframe Transcripts. In Exon Skipping: Methods and Protocols, A. Aartsma-Rus, ed. (Totowa, NJ: Humana Press), pp. 259–271.
28. Garanto, A., Chung, D.C., Duijkers, L., Corral-Serrano, J.C., Messchaert, M., Xiao, R., Bennett, J., Vandenberghe, L.H., and Collin, R.W.J. (2016). In vitro and in vivo rescue of aberrant splicing in CEP290-associated LCA by antisense oligonucleotide delivery. Hum. Mol. Genet. *25*, 2552–2563.
29. Gadgil, A., and Raczyńska, K.D. (2021). U7 snRNA: A tool for gene therapy. J. Gene Med. *23*, e3321.
30. Schümperli, D., and Pillai, R.S. (2004). The special Sm core structure of the U7 snRNP: far-reaching significance of a small nuclear ribonucleoprotein. Cell. Mol. Life Sci. *61*, 2560–2570.
31. Lesman, D., Rodriguez, Y., Rajakumar, D., and Wein, N. (2021). U7 snRNA, a Small RNA with a Big Impact in Gene Therapy. Hum. Gene Ther. *32*, 1317–1329.
32. Flamier, A., Barabino, A., and Bernier, G. (2016). Differentiation of Human Embryonic Stem Cells into Cone Photoreceptors. Bio-protocol *6*, e1870.
33. Huang, D., Heath Jeffery, R.C., Aung-Htut, M.T., McLenachan, S., Fletcher, S., Wilton, S.D., and Chen, F.K. (2022). Stargardt disease and progress in therapeutic strategies. Ophthalmic Genet. *43*, 1–26.
34. Boon, N., Alves, C.H., Mulder, A.A., Andriessen, C.A., Buck, T.M., Quinn, P.M.J., Vos, R.M., Koster, A.J., Jost, C.R., and Wijnholds, J. (2021). Defining Phenotype, Tropism, and Retinal Gene Therapy Using Adeno-Associated Viral Vectors (AAVs) in New-Born Brown Norway Rats with a Spontaneous Mutation in Crb1. Int. J. Mol. Sci. *22*, 3563.
35. Duong, T.T., Lim, J., Vasireddy, V., Papp, T., Nguyen, H., Leo, L., Pan, J., Zhou, S., Chen, H.I., Bennett, J., and Mills, J.A. (2019). Comparative AAV-eGFP Transgene Expression Using Vector Serotypes 1-9, 7m8, and 8b in Human Pluripotent Stem Cells, RPEs, and Human and Rat Cortical Neurons. Stem Cells Int. *2019*, 7281912.
36. Srivastava, A. (2016). In vivo tissue-tropism of adeno-associated viral vectors. Curr. Opin. Virol. *21*, 75–80.
37. Lisowski, L., Tay, S.S., and Alexander, I.E. (2015). Adeno-associated virus serotypes for gene therapeutics. Curr. Opin. Pharmacol. *24*, 59–67.
38. Hori, T., Fukutome, M., and Koike, C. (2019). Adeno Associated Virus (AAV) as a Tool for Clinical and Experimental Delivery of Target Genes into the Mammalian Retina. Biol. Pharm. Bull. *42*, 343–347.
39. Wu, Z., Yang, H., and Colosi, P. (2010). Effect of genome size on AAV vector packaging. Mol. Ther. *18*, 80–86.
40. Surace, E.M., and Auricchio, A. (2008). Versatility of AAV vectors for retinal gene transfer. Vis. Res. *48*, 353–359.
41. Rabinowitz, J., Chan, Y.K., and Samulski, R.J. (2019). Adeno-associated Virus (AAV) versus Immune Response. Viruses *11*.

42. McClements, M.E., Barnard, A.R., Charbel Issa, P., and MacLaren, R.E. (2020). Assessment of AAV Dual Vector Safety in theAbca4(-/-) Mouse Model of Stargardt Disease. Transl. Vis. Sci. Technol. *9*, 20.

43. Colella, P., Ronzitti, G., and Mingozzi, F. (2018). Emerging Issues in AAV-Mediated In Vivo Gene Therapy. Mol. Ther. Methods Clin. Dev. *8*, 87–104.

44. Russell, S., Bennett, J., Wellman, J.A., Chung, D.C., Yu, Z.F., Tillman, A., Wittes, J., Pappas, J., Elci, O., McCague, S., et al. (2017). Efficacy and safety of voretigene neparvovec (AAV2-hRPE65v2) in patients with RPE65-mediated inherited retinal dystrophy: a randomised, controlled, open-label, phase 3 trial. Lancet *390*, 849–860.

45. Maguire, A.M., Bennett, J., Aleman, E.M., Leroy, B.P., and Aleman, T.S. (2021). Clinical Perspective: Treating RPE65-Associated Retinal Dystrophy. Mol. Ther. *29*, 442–463.

46. Girach, A., Audo, I., Birch, D.G., Huckfeldt, R.M., Lam, B.L., Leroy, B.P., Michaelides, M., Russell, S.R., Sallum, J.M.F., Stingl, K., et al. (2022). RNA-based therapies in inherited retinal diseases. Ther. Adv. Ophthalmol. *14*, 25158414221134602.

47. Achberger, K., Cipriano, M., Düchs, M.J., Schön, C., Michelfelder, S., Stierstorfer, B., Lamla, T., Kauschke, S.G., Chuchuy, J., Roosz, J., et al. (2021). Human stem cell-based retina on chip as new translational model for validation of AAV retinal gene therapy vectors. Stem Cell Rep. *16*, 2242–2256.

48. Garita-Hernandez, M., Routet, F., Guibbal, L., Khabou, H., Toualbi, L., Riancho, L., Reichman, S., Duebel, J., Sahel, J.A., Goureau, O., and Dalkara, D. (2020). AAV-Mediated Gene Delivery to 3D Retinal Organoids Derived from Human Induced Pluripotent Stem Cells. Int. J. Mol. Sci. *21*, 994.

49. Inatani, M., Honjo, M., Oohira, A., Kido, N., Otori, Y., Tano, Y., Honda, Y., and Tanihara, H. (2002). Spatiotemporal Expression Patterns of N-Syndecan, a Transmembrane Heparan Sulfate Proteoglycan Developing Retina. Invest. Ophthalmol. Vis. Sci. *43*, 1616–1621.

50. Wishart, T.F.L., and Lovicu, F.J. (2023). Heparan sulfate proteoglycans (HSPGs) of the ocular lens. Prog. Retin. Eye Res. *93*, 101118.

51. Afanasyeva, T.A.V., Corral-Serrano, J.C., Garanto, A., Roepman, R., Cheetham, M.E., and Collin, R.W.J. (2021). A look into retinal organoids: methods, analytical techniques, and applications. Cell. Mol. Life Sci. *78*, 6505–6532.

52. Xue, K., Jolly, J.K., Barnard, A.R., Rudenko, A., Salvetti, A.P., Patrício, M.I., Edwards, T.L., Groppe, M., Orlans, H.O., Tolmachova, T., et al. (2018). Beneficial effects on vision in patients undergoing retinal gene therapy for choroideremia. Nat. Med. *24*, 1507–1512.

53. MacLaren, R.E., Groppe, M., Barnard, A.R., Cottriall, C.L., Tolmachova, T., Seymour, L., Clark, K.R., During, M.J., Cremers, F.P.M., Black, G.C.M., et al. (2014). Retinal gene therapy in patients with choroideremia: initial findings from a phase 1/2 clinical trial. The Lancet *383*, 1129–1137.

54. Cehajic-Kapetanovic, J., Xue, K., Martinez-Fernandez de la Camara, C., Nanda, A., Davies, A., Wood, L.J., Salvetti, A.P., Fischer, M.D., Aylward, J.W., Barnard, A.R., et al. (2020). Initial results from a first-in-human gene therapy trial on X-linked retinitis pigmentosa caused by mutations in RPGR. Nat. Med. *26*, 354–359.

55. Bainbridge, J.W.B., Mehat, M.S., Sundaram, V., Robbie, S.J., Barker, S.E., Ripamonti, C., Georgiadis, A., Mowat, F.M., Beattie, S.G., Gardner, P.J., et al. (2015). Long-term effect of gene therapy on Leber's congenital amaurosis. N. Engl. J. Med. *372*, 1887–1897.

56. Taylor, A.W. (2016). Ocular Immune Privilege and Transplantation. Front. Immunol. *7*, 37.

57. Benhar, I., London, A., and Schwartz, M. (2012). The privileged immunity of immune privileged organs: the case of the eye. Front. Immunol. *3*, 296.

58. Chandler, L.C., McClements, M.E., Yusuf, I.H., Martinez-Fernandez de la Camara, C., MacLaren, R.E., and Xue, K. (2021). Characterizing the cellular immune response to subretinal AAV gene therapy in the murine retina. Mol. Ther. Methods Clin. Dev. *22*, 52–65.

59. Chan, Y.K., Wang, S.K., Chu, C.J., Copland, D.A., Letizia, A.J., Costa Verdera, H., Chiang, J.J., Sethi, M., Wang, M.K., Neidermyer, W.J., Jr., et al. (2021). Engineering adeno-associated viral vectors to evade innate immune and inflammatory responses. Sci. Transl. Med. *13*, eabd3438.

60. Srivastava, A., Mallela, K.M.G., Deorkar, N., and Brophy, G. (2021). Manufacturing Challenges and Rational Formulation Development for AAV Viral Vectors. J. Pharm. Sci. *110*, 2609–2624.

61. Tran, N.T., Heiner, C., Weber, K., Weiand, M., Wilmot, D., Xie, J., Wang, D., Brown, A., Manokaran, S., Su, Q., et al. (2020). AAV-Genome Population Sequencing of Vectors Packaging CRISPR Components Reveals Design-Influenced Heterogeneity. Mol. Ther. Methods Clin. Dev. *18*, 639–651.

62. Goyenvalle, A. (2012). Engineering U7snRNA gene to reframe transcripts. Methods Mol. Biol. *867*, 259–271.

63. Suárez-Herrera, N., Tomkiewicz, T.Z., Garanto, A., and Collin, R.W.J. (2022). Development and Use of Cellular Systems to Assess and Correct Splicing Defects. Methods Mol. Biol. *2434*, 145–165.

64. Vázquez-Domínguez, I., Li, C.H.Z., Fadaie, Z., Haer-Wigman, L., Cremers, F.P.M., Garanto, A., Hoyng, C.B., and Roosing, S. (2022). Identification of a Complex Allele in IMPG2 as a Cause of Adult-Onset Vitelliform Macular Dystrophy. Invest. Ophthalmol. Vis. Sci. *63*, 27.

65. Pan, D., Xia, X.X., Zhou, H., Jin, S.Q., Lu, Y.Y., Liu, H., Gao, M.L., and Jin, Z.B. (2020). COCO enhances the efficiency of photoreceptor precursor differentiation in early human embryonic stem cell-derived retinal organoids. Stem Cell Res. Ther. *11*, 366.

66. Zhou, S., Flamier, A., Abdouh, M., Tétreault, N., Barabino, A., Wadhwa, S., and Bernier, G. (2015). Differentiation of human embryonic stem cells into cone photoreceptors through simultaneous inhibition of BMP, TGFbeta and Wnt signaling. Development *142*, 3294–3306.

67. Green, M.R., and Sambrook, J. (2020). Precipitation of RNA with Ethanol. Cold Spring Harb. Protoc. *2020*, 101717.

68. Livak, K.J., and Schmittgen, T.D. (2001). Analysis of Relative Gene Expression Data Using Real-Time Quantitative PCR and the $2^{-\Delta\Delta CT}$ Method. Methods *25*, 402–408.

69. Schindelin, J., Arganda-Carreras, I., Frise, E., Kaynig, V., Longair, M., Pietzsch, T., Preibisch, S., Rueden, C., Saalfeld, S., Schmid, B., et al. (2012). Fiji: an open-source platform for biological-image analysis. Nat. Methods *9*, 676–682.